

## Magnetoacoustic Oscillations and the Fermi Surface in Aluminum

B. W. ROBERTS

General Electric Research Laboratory, Schenectady, New York

(Received April 11, 1960)

Measurements of magnetoacoustic attenuation in very pure aluminum have been made with 10 to 100 Mc/sec longitudinal sound waves in magnetic fields up to 9200 oe. at a temperature of 4.2°K. The observed oscillations, or geometric resonances, for various crystal and field orientations may be interpreted utilizing the second zone of the nearly free electron Fermi surface model proposed by Harrison. The data suggest regions of high scattering near [100] portions of the surface that prevent the observation of periods for some orbit configurations.

### INTRODUCTION

RECENT theoretical progress<sup>1-3</sup> in the understanding of interactions between sound waves and electrons in very pure metals subject to a magnetic field, as well as new experimental results, promises to yield much new information concerning the band structure of metals.

Bömmel<sup>4</sup> first observed an oscillatory behavior in the ultrasound attenuation as a function of an applied magnetic field. Subsequently, more extensive measurements have been made on tin,<sup>5</sup> copper,<sup>6</sup> lead,<sup>7</sup> and the semimetal, bismuth.<sup>8</sup> Attempts to observe oscillations in aluminum<sup>9,10</sup> have not been successful, apparently because of low purity and the related undesirable short electron mean free path of available single crystals.

Heine<sup>11</sup> has studied the problem of the Fermi surface in aluminum and has proposed possible models of a general nature, while Harrison<sup>12-14</sup> has proposed a more specific surface after study of the pertinent experimental data including: the de Haas-van Alphen effect, cyclotron resonance, the anomalous skin effect, and low-temperature specific heat. From consideration of these data he has proposed that the Fermi surface in aluminum may be taken to a close approximation as that predicted by the nearly free-electron model.

The availability of this new Fermi surface model plus the recent preparation of very pure aluminum has

prompted the following study of magnetoacoustic oscillations and their relationship to the Fermi surface in aluminum.

### EXPERIMENTAL

Ultrasonic pulse techniques similar to those described by Morse<sup>15</sup> were used; a single quartz transducer was arranged for both production and detection of one microsecond pulses.<sup>16</sup> The maximum rf pulse amplitude was 300 volts. The bond between crystal and transducer was made with a very thin layer of "Nonaq," a water soluble stopcock grease, by application of a moderate pressure to the crystal-grease-transducer assembly for two to three hours. The experimental arrangement is shown in Fig. 1.

Three broad band amplifiers<sup>16</sup> of 20 db amplification each were used. The signal produced was rectified and clipped with a simple diode circuit. The pulses reflected from the parallel crystal surfaces were displayed on a cathode-ray oscilloscope. The sample, immersed in liquid He, was held at the end of a rigid metal coaxial line by light spring pressure, and this assembly was suspended in a glass dewar system. The magnetic field was supplied by an electromagnet<sup>16</sup> with pole pieces of 12 in. diameter separated by a 3½-in. gap. The field was very uniform and regulated in the range from approximately 100 to 9200 oe.

After the equivalence of the adjacent pulse comparison and single pulse amplitude methods for measuring relative attenuation was demonstrated, the latter, more convenient technique was used.

The monocrystals were oriented by x-ray diffraction techniques, and the parallel surfaces were oriented within one degree of a major set of planes. The final surface was prepared by first fly-cutting in steps of 0.001 in. and then hand lapping with 600 mesh abrasive papers. A final parallelism of 0.0001 in. over ¾ in. was found desirable for distinct and large reflected pulses.

The aluminum monocrystals were prepared by twelve-pass zone melting under argon by K. T. Aust and J. E. Hilliard of this laboratory. Resistivity ratios ( $R_{25^\circ\text{C}}/$

<sup>1</sup> V. L. Gurevich, J. Exptl. Theoret. Phys. (U. S. S. R.) **37**, 71 (1959) [translation: Soviet Phys.—JETP **37**, 51 (1960)].

<sup>2</sup> T. Kjeldaa, and T. Holstein, Phys. Rev. Letters **2**, 340 (1959).

<sup>3</sup> M. H. Cohen, M. J. Harrison, and W. A. Harrison, Phys. Rev. **117**, 937 (1960). (Many references to related theory.)

<sup>4</sup> H. E. Bömmel, Phys. Rev. **100**, 758 (1955).

<sup>5</sup> T. Olsen and R. W. Morse, Bull. Am. Phys. Soc. **4**, 167 (1959); A. A. Galkin and A. P. Korolyuk, J. Exptl. Theoret. Phys. (U.S.S.R.) **37**, 310 (1959) [translation: Soviet Phys.—JETP **37** (10), 219 (1960)].

<sup>6</sup> R. W. Morse and J. D. Gavenda, Phys. Rev. Letters **2**, 250 (1959); J. R. Neighbours and G. A. Alers, Phys. Rev. Letters **3**, 265 (1959).

<sup>7</sup> Alan Mackintosh (private communication).

<sup>8</sup> D. H. Reneker, Phys. Rev. **115**, 303 (1959).

<sup>9</sup> G. A. Alers and J. R. Neighbours (private communication).

<sup>10</sup> R. W. Morse and H. V. Bohm, *Proceedings of the Fifth International Conference on Low-Temperature Physics and Chemistry, Madison, Wisconsin, August 30, 1957*, edited by J. R. Dillinger (University of Wisconsin Press, Madison, 1958).

<sup>11</sup> V. Heine, Proc. Roy. Soc. (London) **A240**, 340 (1956).

<sup>12</sup> W. A. Harrison, Phys. Rev. **116**, 555 (1959).

<sup>13</sup> W. A. Harrison, Phys. Rev. **118**, 1182 (1960).

<sup>14</sup> W. A. Harrison, Phys. Rev. **118**, 1190 (1960).

<sup>15</sup> R. W. Morse, *Progress in Cryogenics I* (Heywood and Company, Ltd. London, 1959).

<sup>16</sup> Rf pulser, Arenberg Ultrasonic Lab., Inc., Model PG-650-C; Amplifiers: Hewlett-Packard wide band amplifier, Model 460A; Magnet: Varian V4012-3B.

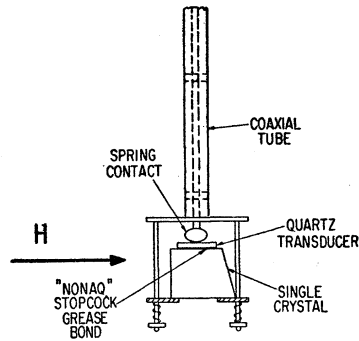


FIG. 1. Schematic of experimental arrangement.

$R_{4.2^\circ\text{K}}$ ) of 8100 were measured on the specimens by the eddy current decay method.<sup>17</sup> This resistivity ratio indicates an electron mean free path on the order of the average sound wavelength utilized in these experiments.

The longitudinal sound velocities were calculated from 0°K values of stiffness moduli<sup>18</sup> obtained by extrapolation of measurements taken at liquid nitrogen temperature and above. The velocities as a function of orientation were [100] 6.75, [110], 6.88, and [111]  $6.92 \times 10^5$  cm/sec.

#### PRESENT THEORY

Pippard<sup>19</sup> first suggested the mechanism for the oscillatory behavior seen in Bömmel's results on tin. He postulated for transverse sound waves that electrons moving under the influence of a magnetic field would interact with sound-wave-induced electric fields which were localized and periodic with the sound wavelength. Thus as the magnetic field was varied and the extremal dimensions of the electron orbits swept through various multiples of the sound wavelength, the sound would be alternately reinforced and attenuated. The period of this oscillatory behavior would relate directly to the Fermi surface.

Kjeldaas and Holstein<sup>2</sup> and Cohen, Harrison, and Harrison<sup>3</sup> have considered the attenuation of longitudinal sound waves in very pure metals subject to transverse magnetic fields. The latter authors used a self-consistent and semiclassical treatment of a sound wave attenuated by a free electron gas in a positive background and predict the falling field-dependent attenuation for long mean free paths shown in Fig. 2. A periodicity is present when the relative attenuation is plotted proportional to  $1/H$ , ( $qR = 2\pi\hbar kc/\lambda eH$ ). Here  $q$  is the sound wave vector ( $2\pi/\lambda$ ),  $R$  is the cyclotron orbit radius, and  $\hbar k$  the momentum of the electron. The conditions are that  $\omega_c\tau \gg 1$ ,  $ql \gg 1$ , and  $\beta \ll 1$  where  $\omega_c$  is the angular cyclotron frequency,  $\tau$  is the relaxation time,  $l$  is the mean free path and  $\beta = \delta/\lambda$  where  $\delta$  is the classical skin depth. Not all of these conditions are attainable

<sup>17</sup> C. P. Bean, R. W. DeBlois, and L. B. Nesbitt, J. Appl. Phys. **30**, 1976 (1959). The measurements were kindly carried out by P. G. Frischmann and T. A. Ross, Jr.

<sup>18</sup> P. M. Sutton, Phys. Rev. **91**, 816 (1953).

<sup>19</sup> A. B. Pippard, Phil. Mag. **2**, 1147 (1957).

because of finite mean free paths in metals and the difficulty of experimentally measuring the attenuation when sound frequencies become large. Kjeldaas and Holstein have considered the intermediate case for  $ql$  on the order of 3 to 15. The result is a reduction in the saturation attenuation at high fields, a damping out of the oscillations, but no appreciable shift in the positions of the maxima as  $ql$  is reduced. The zero field attenuation equals the saturation value when  $ql = 5\pi/2$  and reverses; i.e., the saturation attenuation becomes less than the zero-field value when  $ql < 5\pi/2$ .

The separation of maxima are found to be  $qR = \pi$  at large  $qR$  or small  $H$  and thus

$$\hbar k = \frac{\lambda e}{2c \Delta(1/H)},$$

where  $\mathbf{k}$  is an extremal distance to the Fermi surface, to be discussed later, which may be considered perpendicular to  $\mathbf{q}$  and  $\mathbf{H}$  for the longitudinal wave case because of the 90° rotation between electron paths on the Fermi surface and the real space orbits. Thus the periods  $\Delta(1/H)$  deduced from adjacent maxima relate to dimensions on the Fermi surface, and the over-all shape of the attenuation-reciprocal field curve gives information on the metal purity.

Harrison<sup>20</sup> has considered the theoretical positions of maxima at small  $qR$ . A shift of the maxima by about  $3\pi/8$  towards large  $qR$  is predicted for a spherical Fermi surface in the very long mean free path case. To illustrate the magnitude and trends of the shift, the data of Cohen, Harrison, and Harrison<sup>3</sup> are listed in Table I.

It is noted that the entire series of maxima is shifted to high  $qR$  (minima to low  $qR$ ) and that the largest variation in the  $\Delta(qR)$  occurs for small  $qR$ . These

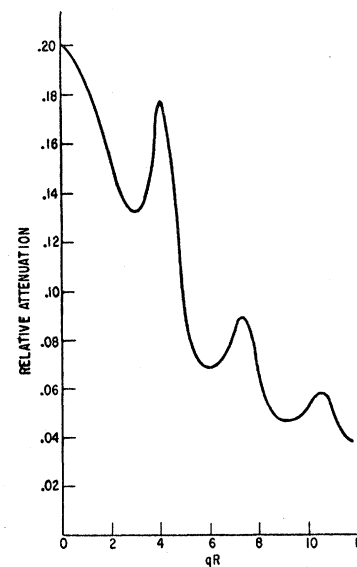


FIG. 2. Predicted longitudinal sound wave attenuation of  $\mathbf{H} \perp \mathbf{q}$ ,  $qR = 2\pi\hbar kc/\lambda eH$  (after Cohen, Harrison, and Harrison, see reference 3).

<sup>20</sup> W. A. Harrison (private communication).

maxima shifts have been observed in the measurements of Morse and co-workers<sup>21</sup> on copper single crystals where ten or more maxima are visible for certain orientations.

Harrison<sup>20</sup> finds that the shift of the maxima depends upon the sign of the curvature of the Fermi surface and should be reversed in the case of aluminum for the second zone, since the surface surrounds a region of holes and is therefore largely concave outward. He also suggests that the presence of other carriers and the scattering may effect the position of the first few maxima in an undetermined manner. A multitude of complex orbit shapes and sizes contributing to the same attenuation curve would tend to broaden the first maximum.

The interaction of the electron with the sound wave disturbance arises largely through the induced electric field which varies sinusoidally in space. Thus electrons traveling around a complex orbit will see a fluctuating electric field. A major contribution to the electric current will arise from those portions of the electron orbits which are perpendicular to  $\mathbf{q}$  and thus corresponding electrons remain in phase with the sound wave and the electric field for an appreciable time. The distance along  $\mathbf{q}$  between two such segments on an orbit represents a measurable dimension of the orbit. If such an orbit corresponds to an extremal portion of the Fermi surface such that adjacent orbits have the same measurable dimension, large amplitude oscillations will be seen, providing the scattering is small. It is difficult to predict the exact oscillatory behavior for a given orbit shape and extremal conditions, although Harrison<sup>20</sup> has arrived at an approximate scheme which gives good agreement. An example is given later. Computation of the contributions from all the orbits participating on a complex surface is a formidable problem.

#### FERMI SURFACE MODEL

The data presented here will be interpreted in terms of the free electron model deduced by Harrison<sup>12,13</sup> and

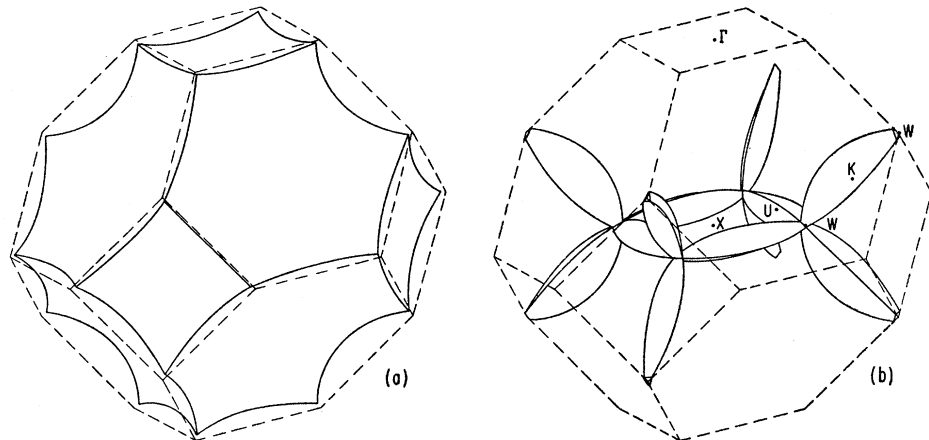


FIG. 3. Nearly free electron Fermi surface in Al after Harrison (see references 12 and 13). (a) Regions of holes in second zone; (b) Regions of electrons in third zone.

TABLE I. Magnitude of  $qR$  at extrema of Fig. 3.

Maxima	$\Delta(qR)$	Minima	$\Delta(qR)$
0		2.94	
4.04	(4.04)	6.04	(3.10)
7.27	(3.23)	9.16	(3.12)
10.45	(3.22)	12.28	(3.12)
13.61	(3.21)	15.41	(3.13)
16.77	(3.16)	18.55	(3.14)
19.92	(3.15)	21.68	(3.13)

shown in Fig. 3. He proposes a filled first zone and in the reduced zone scheme a continuous surface surrounding a pocket of holes in the second zone. The third zone, with origin translated along  $\Gamma X$ , has an interrelated set of arms with varying cross section. The fourth zone contains small pockets of electrons which probably do not occur in the real metal.<sup>13</sup>

Magnetoacoustic oscillations would be expected for many orientations of crystal, field and sound direction due to the complex nature of the second zone surface. The small diameters of the third zone arms give long periods which are difficult to detect. It is highly unlikely that the orbits lying inside the ring structure of the third zone will be seen due to the small number of electrons participating. These orbits, denoted "ξ," have been observed ultrasonically in lead by Mackintosh<sup>7</sup> where the arms are much larger in cross section.

#### EXPERIMENTAL RESULTS

The attenuation as a function of field was measured at a variety of frequencies from 10 to 100 Mc/sec with useful data occurring in the range 40 to 70 Mc/sec. All measurements reported here are for longitudinal waves utilizing X-cut quartz plates, although attempts were made to observe the oscillations with transverse waves (AC-cut quartz plates). The latter were unsuccessful, due to a very large total attenuation at low temperature.

Preliminary measurements of the attenuation frequency dependence are shown in Fig. 4. The sound wave

<sup>21</sup> R. W. Morse (unpublished).

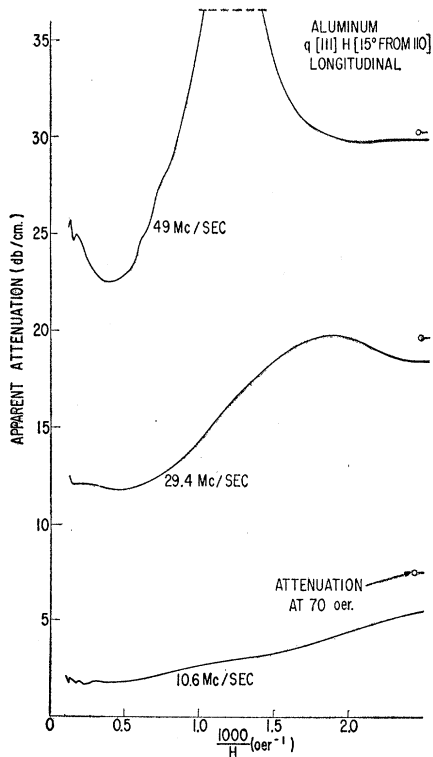


FIG. 4. Ultrasound attenuation in aluminum as a function of frequency at 4.2°K. Transducer, bond, and end losses are included.

number  $q$  lies along a  $[111]$  direction with  $H$  normal to  $q$  and  $15^\circ$  from a  $[110]$  direction. The low field attenuation is nearly linear with sound frequency as predicted by Pippard's free electron theory<sup>22</sup> for the case  $ql \geq 1$ , which gives

$$\alpha \approx \frac{\pi N m v_0 \omega}{6 \rho v_s^2},$$

where  $N$  is the number of electrons per unit volume,  $m$  the electron mass,  $v_0$  the Fermi velocity,  $\omega$  the angular sound frequency,  $\rho$  the density and  $v_s$  is the velocity of sound. The dependence of attenuation on the number of carriers is qualitatively observed in the much larger attenuations observed for aluminum as compared to equivalent measurements in copper. A single oscillation is observed at the higher sound frequency and is seen to move to lower fields as the frequency is reduced as expected for the longer wavelength. The oscillation amplitude also decreases rapidly with frequency.

#### $q$ Along $[110]$

Data were accumulated for the three major crystal orientations. We will discuss first the arrangement with  $q$  propagating along a  $[110]$  direction with  $H$  always applied perpendicular to  $q$ . The two-fold symmetry

<sup>22</sup> A. B. Pippard, *Phil. Mag.* 46, 1104 (1955).

present when the sample is rotated around  $q$  in fixed  $H$ , as well as changes introduced by frequency variation, are shown in Fig. 5. For orientations  $q[110]H[001]$  and  $q[110]H[110]$ , no oscillatory behavior is evident (see Fig. 6). It is noted that the saturation value is lower than the zero field value but is rising for  $H$  above 2000 oe and thus is consistent with  $ql \geq 1$ . These two orientations would be expected to yield periodic maxima with the shortest possible periods, since they would result from the largest orbits available on the second zone surface.

Definite oscillatory behavior was found in the vicinity of  $q[110]H[111]$  and survey measurements as a function of orientation around  $q$  are plotted in Fig. 7. A maximum in the relative attenuation develops when  $H$  lies  $45$  to  $50^\circ$  from  $H[110]$ . A detailed measurement taken at the angle for the largest maximum amplitude is shown in Fig. 8. Two maxima are present, and the inset sketch (a) shows their approximate appearance determined by subtracting off the background attenuation. It is clear that the second maximum is a small fraction of the amplitude of the first. The period  $\Delta(1/H)$  between the origin and the first maximum and that between the first and second maxima are each about  $0.7 \times 10^{-3} \text{ oe}^{-1}$  in contradiction to the  $\sim 4:3$  ratio expected for regions of electrons or the reverse for regions of holes as suggested by Harrison.

Using the direct relationship between periods and Fermi surface dimension, the above period corresponds to  $|k| = 0.71k_0$  where  $k_0 = 2\pi/a_0 = 1.55 \times 10^{-8} \text{ cm}^{-1}$  for aluminum and represents the distance in wave number space from origin to zone boundary equivalent to  $\Gamma X$  in Fig. 4.

To better visualize the extremal dimension indicated

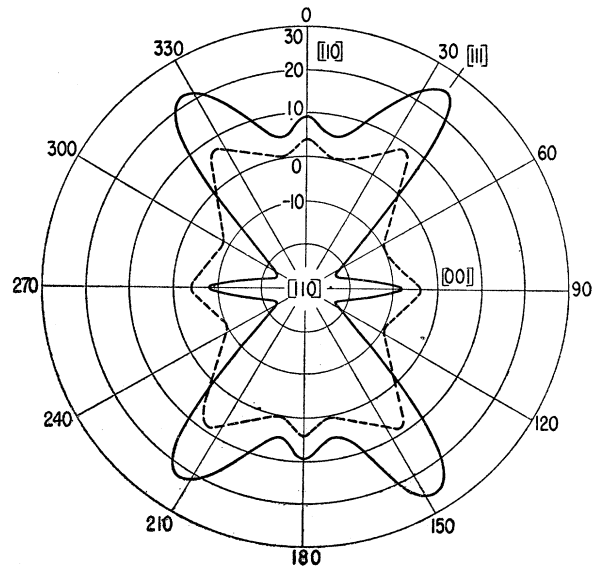


FIG. 5. Attenuation of sound for Al crystal rotated around  $q[110]$  in a fixed field at two frequencies. (Solid curve 66.8 Mc/sec. Dashed curve 44.8 Mc/sec.)

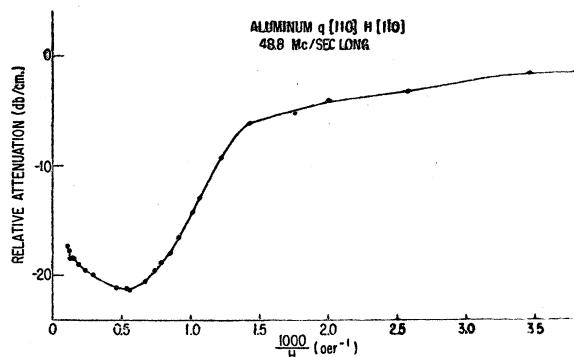


FIG. 6. Ultrasound attenuation in Al for the orientations  $q[110]H[110]$ . The relative attenuation is scaled to the frequencies.

by the maxima, a set of contour lines of the second zone surface are plotted in Fig. 9 in units of  $k_0$ . The measured  $\mathbf{k}$  is plotted for the orientation giving the largest and most distinct maxima. The first point of interest is that the orbits are related to travel on the  $[111]$  portions of the surface (six-sided concave faces) for this arrangement. The fact that the largest amplitude maxima are not observed when the extremal dimension is orthogonal to the six-sided surfaces suggests that electron scattering is high over the four-sided portions of the surface, and a small rotation of the central orbit plane increases the number of participating electrons, although they are not moving on orbits giving the precise extremal dimension. The position of the maximum shown in Fig. 7 moves so as to suggest an increase in  $\mathbf{k}$  as  $\mathbf{H}$  is rotated towards  $[110]$ . However, the complexity of the situation may yield other causes for the broadening and shift of this maximum. No oscillations are observed for  $q[110]H[001]$  and  $q[110]H[1\bar{1}0]$  as would follow for the postulated high scattering on the four-sided surfaces.

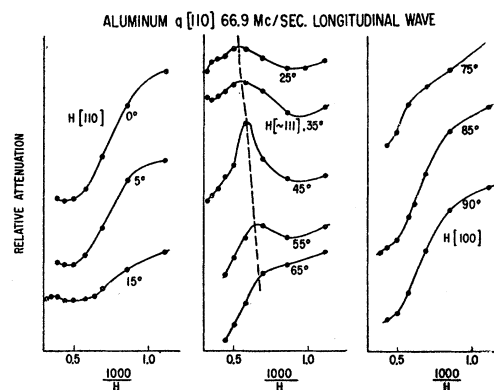


FIG. 7. Survey of magnetoacoustic attenuation in Al for  $q[110]$  to demonstrate first maximum position, amplitude and shift.

The cross section denoted  $AA'$  in Fig. 9 is shown at the top of Fig. 10. The six segments lie on six-sided surface pieces and correspond to the real space orbits of the electrons showing the pronounced oscillations for the  $q[110]$  orientation. Assuming a narrow band of orbits, Harrison<sup>20,23</sup> has indicated that an approximate determination of the location of the positions of the maxima may be made by finding the maxima of  $G(q')$ .

$$G(q') = \left[ \oint \cos q' k_y dk_s \right]^2,$$

where  $q' = qe\hbar/eH$ . This is a line integral in wave-number space around the orbit giving rise to the oscillation; it is assumed that the orbit has a center of symmetry and that  $k_y$  is measured perpendicular to  $\mathbf{q}$  and to  $\mathbf{H}$ . For a circular orbit, this would become

$$G(q'(H)) = (2\pi k_F)^2 J_0^2(qR(H)),$$

$J_0$  being a Bessel function and  $R(H)$  being the orbit

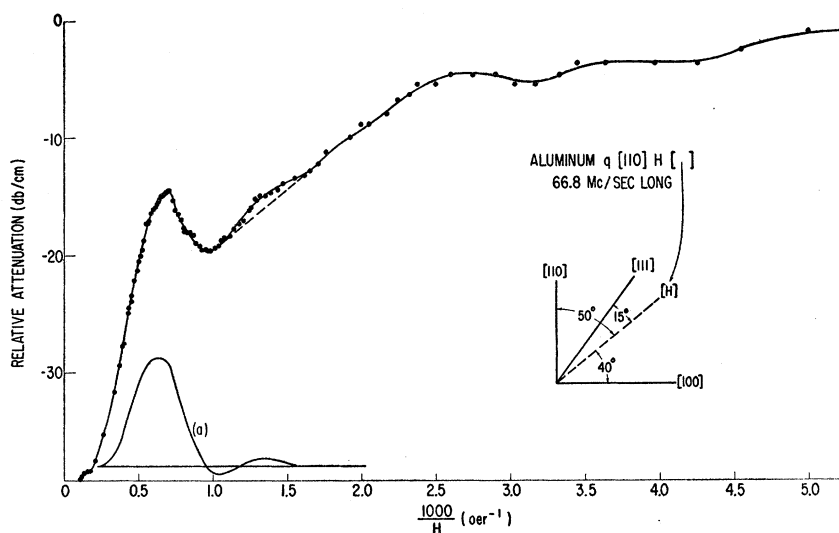


FIG. 8. Ultrasound attenuation in Al for  $q[110]H[50^\circ \text{ from } 110]$ . Curve (a) shows maxima on flat background.

<sup>23</sup> M. J. Harrison, Phys. Rev. Letters 1, 442 (1958).

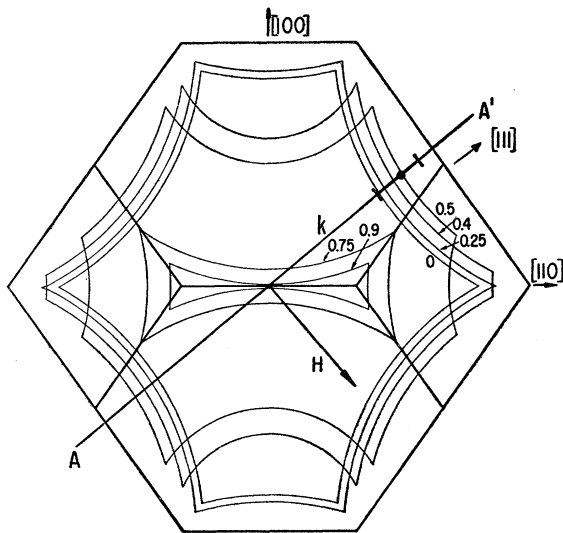


FIG. 9. Contours representing sections taken  $\perp$  to  $[110]$  of second zone. Levels in units of  $k_0$ .

radius in real space and a function of field. If we were to treat the central orbit of a spherical Fermi surface in this way, we would include two thirds of the  $3\pi/8$  low-field phase shift discussed above. Such an analysis, though crude, should give some idea of the location of the peaks. The function  $G(q')$  is plotted in Fig. 10 and yields maxima which agree, probably fortuitously, with the observed maxima positions. The second maximum amplitude has decayed relatively little in amplitude contrary to experiment. The close agreement may be due to the large portion of the orbit which is in phase or in the vicinity of the extremal portion of the curve.

#### $q$ Along $[111]$

Oscillatory behavior was present for all perpendicular orientations of  $\mathbf{H}$  around  $q[111]$ . The attenuation curves for two orientations are shown in Fig. 11. Two related maxima are present, the first having a peak value so high as to be unobservable at 66.8 Mc/sec. Data taken at 49.0 Mc/sec yielded the same two maxima; however, the attenuation was lower and the entire first maximum was observed and found to be symmetrical near the peak. It is also to be noted that the high field attenuation behaves differently for the two orientations. The near-saturation and zero-field attenuations of the  $q[111]\mathbf{H}[15^\circ \text{ from } \bar{1}10]$  are nearly the same, and the steeply rising portion of the curve suggests that the saturation value will be considerably above the zero-field value as predicted for large  $ql$ .

The electron orbits suggested on the second zone surface appear to give extremal dimensions close to those indicated by the periods provided the condition of high scattering is retained for the four-sided portions of the surface. Figure 12 gives the top set of contour lines for the second zone. Note that the lower set of contour lines

must be rotated  $60^\circ$  with respect to the top set. The orbit shapes matching two possible orientations are shown in Fig. 12 (top) along with the indicated dimension from the measured periods. The complexity of the surface appears on visual study to permit orbits with extremal dimensions close to the period dimension observed for all orientations providing the four-sided portions are avoided. A definite but small trend is observed in maxima position as  $\mathbf{H}$  is rotated  $30^\circ$  from a  $[1\bar{1}0]$  direction which appears to correspond to the surface construction. Better data are required before this shift may be used for detailed surface study.

The  $q[111]$  data taken at 66.8 Mc/sec indicate a period from origin to first maxima approximately 10% larger than that measured between the first and second maxima. All other pairs of maxima, including those of other orientations, gave the same periods within experimental error. These observations disagree with the limiting theory for positions of the first few maxima, as well as being opposed with respect to the origin to first maximum period for the region of holes. These disagreements might be resolved and understood by the extension of theory and observations on purer metal specimens.

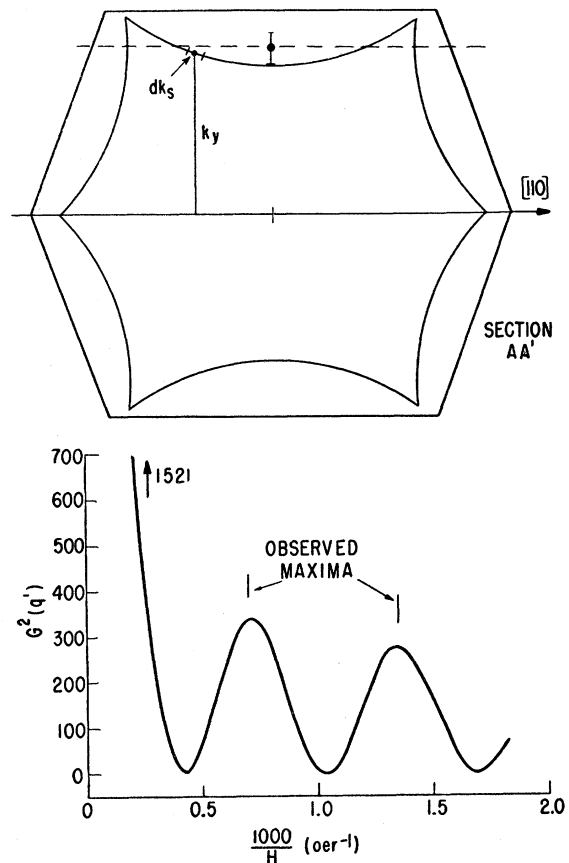


FIG. 10. Cross section of electron orbits giving rise to  $q[110]$  oscillations along with observed and calculated maxima positions. Section  $AA'$  relates to Fig. 9.

**q Along [100]**

The sample orientation with **q** along [100] shows interesting results despite the lack of resolution. Only one broad maximum was usually present as shown in Fig. 13. If the period determined from infinite field to the first maximum is used for a measure of **k**, the extremal dimensions obtained are shown in Fig. 14. The estimated error limits are large because of the presence of only one broad maximum.

For **q**[100]**H**[010] the extremal dimension is given as (a) on Fig. 14, and appears to be related to orbits running around the four-sided area in the plane of the drawing. The shortness compared to the drawn cross section extreme may be related to the rounding off of the sharp intersections as predicted by the more complete theory of Harrison.<sup>13</sup>

For the orientation **q**[100]**H**[011], **k** is measured at the outer portion of the squared neck as at (b), and the orbits are much larger in total size, since they pass entirely around the surface but in such manner as to avoid traversing any four-sided portion of the surface.

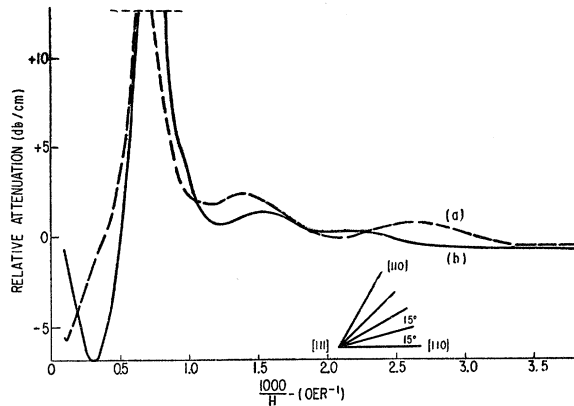


FIG. 11. Ultrasound attenuation in aluminum for case (a) **q**[111]**H**[110] and (b) **H**[15° from 110] for longitudinal waves at 66.8 Mc/sec.

With **H** rotated 11° from [110] the dimension from the period is slightly larger and would be related to the position (c).

The only asymmetric orbit which appears to be present in these data is that illustrated in cross section **AA'** and dimension (d) of Fig. 14. Again the high-scattering conditions of the four-sided surfaces is observed except that at one extreme the orbit would pass over the corner of such a surface. This is the largest dimension indicated by a period. The significance of such orbits, if true, is great since they would make unlikely any contact of the zone surface around the edges of the four-sided area.

**CONCLUSION AND DISCUSSION**

Despite the very complex nature of the interaction of a sound wave with conduction electrons in a very pure

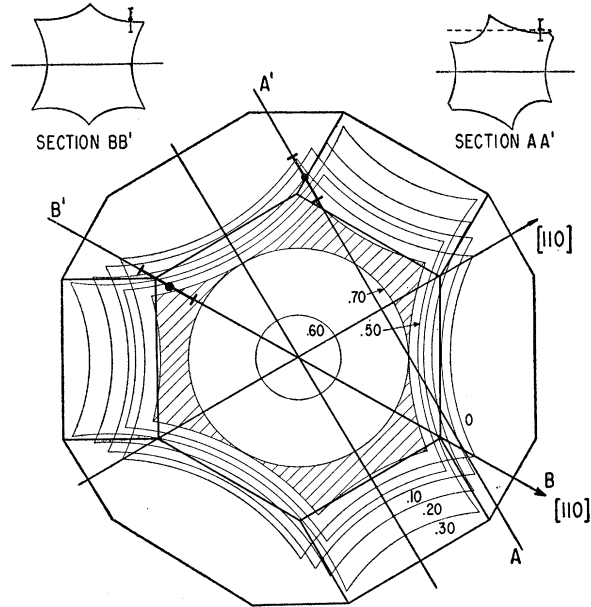


FIG. 12. Contours representing sections taken  $\perp$  to [111] of second zone surface. Levels in units of  $k_0$ . Orbits are sketched for two sections, **AA'** for **q**[111]**H**[110] and **BB'** for **q**[111]**H**[30° from 110].

metal at low temperature, the described observations of magneto-acoustic oscillations in aluminum clearly support the nearly free electron model of the Fermi surface for aluminum proposed by Harrison.<sup>12,13</sup> All oscillations which are observed for low  $qR$  may be interpreted in terms of electron orbits associated with the second zone pocket of holes. However, the lack of oscillations in certain orientations suggests the exclusion of electron orbits passing directly over any of the four-sided second zone surface portions. Since orbit dimensions of nearly the same size as those excluded are observed, it is un-

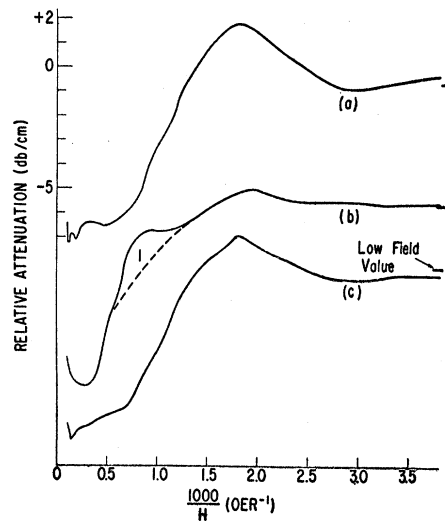


FIG. 13. Ultrasound attenuation in Al for orientations of **H** around **q**[100].

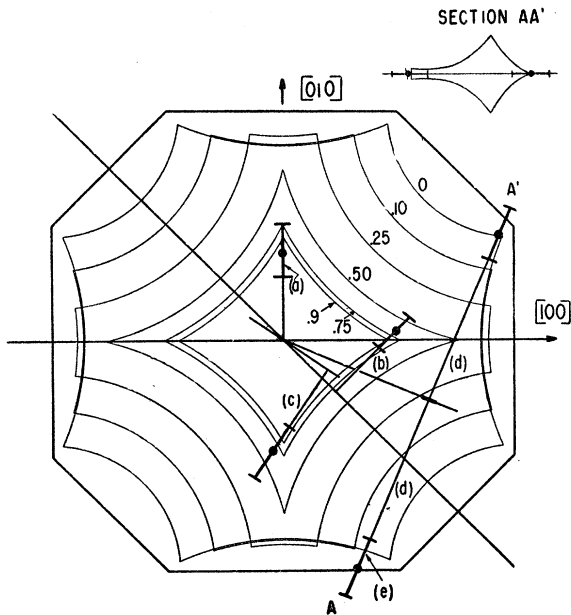


FIG. 14. Contours representing sections taken  $\perp$  to  $[100]$  of second zone surface. Levels in units of  $k_0$ . Indicated dimensions for  $\mathbf{q}[100]$  and (a)  $\mathbf{H}[010]$ , (b)  $\mathbf{H}[011]$ , (c)  $\mathbf{H}[11^\circ \text{ from } 011]$  and (d)  $\mathbf{H}[22\frac{1}{2}^\circ \text{ from } 011]$ .

likely that the magnetoacoustic technique is inoperative here. This leads to the necessity of postulating higher scattering in the regions of the four-sided portions of the surface than that existing on the six-sided portions. It is noted that the four-sided portion of the surface lies closest to the zone faces and thus would permit scattering events with small changes in wave number to lead to large deflection of electrons orbiting in the region and the consequent reduction or removal of the attenuation oscillations. It is possible that these orbits may be observed with aluminum of higher purity.

It is of interest to note the analysis by Roberts<sup>24</sup> of the complex dielectric constant determined by light reflection methods. He finds that at least two electron relaxation times are required for aluminum in accord

<sup>24</sup> S. Roberts (private communication). A similar analysis is given for Ni in Phys. Rev. **114**, 104 (1959).

with the present requirement of high scattering on one set of surfaces.

The suggestion of the asymmetric orbit of Fig. 14 permits electrons to make short trajectories over the high scattering regions without being unduly scattered. The presence of this orbit would exclude Fermi surface models discussed by Heine<sup>18</sup> and Harrison<sup>9</sup> that include contact of the zone surface near the edges of the four-sided surface.

The alternate model suggested by Heine<sup>18</sup> in which the second zone pocket of holes touches all edges of the zone would be excluded by the observed oscillations related to orbits passing around on six-sided portions of the surface as shown in the  $\mathbf{q}[110]\mathbf{H}[50^\circ \text{ from } 110]$  experiment.

The extended band calculations of Harrison<sup>13</sup> predict small modifications from the single-OPW or nearly free electron Fermi surface which are not of importance here. The additional terms cause the rounding off of the sharp edges of the Fermi surface in the second zone but no major shifts in surface dimensions.

The conclusions drawn from these data must be regarded in the light of experimental conditions which are less favorable than those observed in magnetoacoustic studies of other pure metals such as copper<sup>6</sup> and lead<sup>7</sup> where many oscillations are observed and more accurate periods are thus available. The few oscillations observed with these aluminum specimens of intermediate  $ql$  plus the present indeterminacy in relating the first maximum position to the extremal dimension in  $\mathbf{k}$  space also requires caution in utilizing the indicated detailed dimensions.

#### ACKNOWLEDGMENTS

Very helpful discussions with H. E. Bömmel of Bell Telephone Laboratories and R. W. Morse of Brown University are acknowledged. Some aluminum samples were kindly supplied by J. W. Rutter of this laboratory.

The author is greatly indebted to his colleagues for much advice and encouragement, especially E. H. Jacobsen, L. B. Nesbitt, and J. R. Young for equipment design, and to W. A. Harrison for continuous enlightenment on theoretical interpretation and his many contributions noted in the text.